



Fixed-bed column adsorption of carbon dioxide by sodium hydroxide modified activated alumina

M. Auta^{a,c}, N.D. Amat Darbis^a, A.T. Mohd Din^a, B.H. Hameed^{a,b,*}

^aSchool of Chemical Engineering, Engineering Campus, Universiti Sains Malaysia, 14300 Nibong Tebal, Penang, Malaysia

^bChemical Engineering Department, College of Engineering, King Saud University, P.O. Box 800, Riyadh 11421, Saudi Arabia

^cDepartment of Chemical Engineering, Federal University of Technology, Minna, Nigeria

HIGHLIGHTS

- Activated alumina was modified with 30% NaOH and calcined at 500 °C for 4 h (3MAA).
- Physical and chemical characterization of the adsorbents were carried out.
- Carbon dioxide was adsorbed from CO₂/N₂ mixture in a continuous adsorption system.
- Regeneration of the 3MAA were successfully tested for three cycles.

ARTICLE INFO

Article history:

Received 22 May 2013

Received in revised form 2 August 2013

Accepted 5 August 2013

Available online 11 August 2013

Keywords:

Breakthrough

Carbon dioxide

Adsorption

Activated alumina

Mesoporous

ABSTRACT

Activated alumina was successfully modified with sodium hydroxide (NaOH) and used for capturing of CO₂ in fixed-bed column adsorption system. Calcinations temperature (200–500 °C), time (2–4 h) and concentration of NaOH (10–40%) suitable for the modification were studied. Surface area and porosity, morphology/elemental composition, crystal structure and functional groups of the plain activated alumina (PAA) and optimally modified adsorbent with 30% NaOH calcined at 500 °C for 4 h (3MAA) were characterized using nitrogen adsorption–desorption, scanning electron microscopy/energy dispersive X-ray, X-ray diffraction and Fourier transform infrared spectroscopy techniques (4000–500 cm⁻¹). The effect of CO₂ % in the feed, adsorption temperature, 3MAA particle sizes, feed flow rate and amount of 3MAA in the column were investigated in the adsorption experiments. Adsorption capacity of 3MAA and PAA were 51.92 and 19.61 mg/g even with their surface areas of 203 and 207 m²/g, respectively. The enhanced adsorption on 3MAA was due to its average pore width and total pore volume which were larger than those of PAA. Physisorption activities that characterized the nature of the 3MAA adsorption, enhanced easier desorption of CO₂ conveniently for three cycles. The results of this study have revealed that sodium hydroxide modified activated alumina can be applied for CO₂ pollution control in the environment.

© 2013 Elsevier B.V. All rights reserved.

1. Introduction

There is a necessity for more proactive action in tackling air pollution since it is a more global challenge than other forms which can be localized. Air occupies the entire universe and has its pollutants along with it. Carbon dioxide (CO₂) among other air pollutants is a major culprit to the greenhouse gases that is fueling global warming. It can be sourced from aerospace industry, hydrogen gas production, hydrocarbons purification, treatment of natural gas and a major source like fossil fuel which accounts for 25 billion tons that is released to the atmosphere annually [1,2].

* Corresponding author at: School of Chemical Engineering, Engineering Campus, Universiti Sains Malaysia, 14300 Nibong Tebal, Penang, Malaysia. Tel.: +60 45996422; fax: +60 45941013.

E-mail address: hbassim@eng.usm.my (B.H. Hameed).

And presently, the world energy source is largely dependent on fossil fuel with cleaner greener renewable alternative energy sources still in developmental stages [3]. The need to contain CO₂ emission aside guiding against the greenhouse effect, is to aid in accomplishing absolute air and natural gas purification amongst others.

Measures such as zero CO₂ emission technologies, point source capture and sequestration are attempts made to check CO₂ pollution effect [4]. New plants with zero CO₂ emission have also attempted using membrane science, cryogenic distillation, solvent absorption, fixation using algae and adsorption methods with a view to salvaging the pollution challenge [4,5]. The high efficiency, affordable energy and application of less resources using adsorption for CO₂ capture has made the process outstanding from others [2,6].

Various adsorbents such as hydrotalcite and inorganic-porous materials, activated carbons, basic oxide and amine-based have been employed in catalysis and adsorption of CO₂ pollutant from the environment [7–10]. But some of these adsorbents like the amine based require high energy and possess degradation threat through oxidation that results in corrosion [11]. Some commercial adsorbents have low selectivity and low capability of CO₂ adsorption [3].

In the quest for more efficient and effective CO₂ capturing adsorbents, few studies have been conducted on the use of transition, activated and modified alumina. But it has been proven that on the surface of alumina lies chemical and physical active sites that has affinity for CO₂ molecules [6,12,13]. This may be attributed to alumina amphoteric nature that is the ability to withstand or dissolve in both acid and base solution [14].

In this work a cost effective, low energy intensity, environmental friendly and high capacity adsorbent from activated alumina for CO₂ adsorption was developed. The carbon dioxide was adsorbed from a mixture of CO₂/N₂ since flue gas emissions are often associated with considerable amount of nitrogen gas [15]. The percentage of sodium hydroxide (NaOH) used for modification, calcinations temperature and time were studied. The fixed-bed adsorption experiment involved study of the effect of some process parameters such as effect of flow rate, bed height and influent CO₂ concentration, adsorbent particle size and adsorption temperature on the breakthrough curves.

2. Materials and methods

2.1. Materials

Activated alumina of 1–2 mm particle sizes was supplied by OMI (M) Sdn. Bhd., Malaysia. Sodium hydroxide was purchased from Mercks Chemical company, while purified carbon dioxide (99.9%) and nitrogen (99.9%) gases were supplied by Wellgas Sdn. Bhd., all in Malaysia.

2.2. Preparation of CO₂ adsorbent

The activated alumina beads were slightly washed with distilled water and dried in an oven at 110 °C for 6 h. The dried beads were packaged in air tight container and used as unmodified or plain activated alumina (PAA) adsorbent.

Ten grams of unmodified activated alumina was treated with 30 mL of different concentration (10–40%) of NaOH and allowed to dwell for 2 h. The treated unmodified activated alumina beads according to the percentage of NaOH used were designated as follows: 1MAA, 2MAA, 3MAA and 4MAA for 10%, 20%, 30% and 40%, respectively. Afterwards, the NaOH solution was decanted from the beads and then dried in an oven at 110 °C for 6 h before calcinations at various temperatures (200–500 °C) and time (2–4 h) [16]. Excess sodium on the surface of the adsorbent was evacuated by washing with distilled water while monitoring the pH after which it was dried and packaged for further use [17,18].

2.3. Fixed-bed column adsorption

The adsorbent was measured into the adsorption column and dried by heating to 110 °C under an inert atmosphere and allowed to dwell for 1 h before cooling to the desired adsorption temperature. A mixture of high purity nitrogen gases was passed through an adsorption column of length 42 cm and a diameter of 1.1 cm in an upward flow. The inflow of each gas from the cylinders were controlled by a calibrated mass flow controller AALBORG (model AFC26 NY, USA). The amount of CO₂ adsorbed after every 10 s

was determined by an online carbon dioxide analyzer model 906 (Quentek instrument, USA).

The effect of adsorption parameters such as percentage of CO₂ in the feed stream, flow rate, adsorption temperature and bed depth were studied. The percentage of CO₂ in the feed stream varied from 12%, 15% and 18%; the influent flow rate of 90, 120 and 150 mL/min; 35(±), 45(±) and 55(±) °C were the temperatures varied for the adsorption process; and the amount of adsorbent (PAA and MAA) were 2, 4 and 6 g.

The adsorption experimental breakthrough curves were generated by the Carbon dioxide analyzer and relayed in the desktop computer attached to it.

2.4. Regeneration of adsorbent

At the end of an adsorption process, the adsorption column with the adsorbent fixed on it was heated up to 110 °C for 1 h under nitrogen gas flow to desorb molecules of CO₂ adsorbed on the 3MAA surface. The stability of desorption was ascertained by passing the column exit gas through the CO₂ analyzer until the residual CO₂ concentration was steady. The column was purged using a vacuum pump for 30 min to remove the trapped gas in the adsorbent. Then another cycle of CO₂ adsorption was carried out and similar procedure was repeated for three cycles of adsorption–desorption. During the reusability test, the column conditions such as adsorption temperature (35 °C), percentage of CO₂ (15%) in the feed (85% balance of N₂), total feed flow rate (90 mL/min), amount of adsorbent used (4 g) and adsorbent size (1–2 mm) were kept constants.

2.5. Characterization of adsorbents

The PAA and 3MAA surface area and porosity were determined by Brunauer–Emmett–Teller (BET), morphology and elemental composition using scanning electron microscopy and Energy-dispersive X-ray spectroscopy technique. The crystal structure and functional groups of the adsorbents were analyzed using X-ray diffraction and Fourier transform infrared spectroscopy techniques, respectively.

An autosorb Brunauer–Emmett–Teller Micrometric ASAP 2020 operating with the static volumetric technique was used to determine the surface area and porosity of the adsorbent. Samples were degassed at 300 °C for 2 h measurement of equilibrium pressure of a known volume of liquid nitrogen for the generation of adsorption–desorption isotherms. Barrett–Joyner–Halenda and t-plot method were used to evaluate the average pore size distribution cum total pore volume, respectively while the BET equation was used to calculate the surface area.

An integrated scanning electron microscopy (SEM) and energy dispersive X-ray (EDX) microanalysis (Oxford INCA 400, Germany) was used to determine the physical morphology and chemical composition of plain and modified activated alumina adsorbent. The bead samples were attached to an aluminum stub with a carbon tape before placement in the analyzer chamber for scanning.

A Siemens XRD D5000 diffractometer that is equipped with Cu K α radiation at a beam voltage of 40 kV with a scanning rate of 2° per minute recording between 5° and 90°, was used to determine the crystal structure of unmodified and modified activated alumina adsorbents. The small glancing angle was fixed at 2 θ .

Fourier transform infrared spectroscopy (FTIR) analysis was applied to determine the surface functional groups on the adsorbents. After 100 times of scans, spectra between 4000–400 cm⁻¹ were taken using potassium bromide (KBr) as the mulling agent. Both the KBr and samples were dried overnight in an oven at 110 °C before mixing together in a 5% adsorbent and balance KBr. A 7 mm diameter of 1 mm thickness was formed with the aid of hydraulic press prior to analysis.

3. Results and discussion

3.1. Characterization of adsorbent

The BET quantitative analysis and nitrogen adsorption–desorption isotherms for surface area and porosity of PAA and 3MAA are presented in Table 1 and Fig. 1, respectively.

Modification of the activated alumina with 30% NaOH (3MAA) was observed to have affected the surface area of the activated alumina. A decrease of $3.82 \text{ m}^2/\text{g}$ occurred which was attributed to structural changes of the adsorbent according to the XRD results. A similar observation has been reported on decrease in surface area after modification and successful calcinations of a catalyst [19]. However, the structural changes after modification increased the total pore volume and average pore width as can be seen in Table 1. The nitrogen adsorption–desorption isotherms plots of the activated alumina adsorbent before and after modification were both mesoporous and of type IV isotherm according to IUPAC classification. This signified a monolayer-multilayer adsorption nature of the adsorbent [20].

The morphological structure of the PAA revealed the interconnected structure of the alumina even though it was bare when compared with the wrinkled 3MAA surface as shown in Fig. 2. The emergence of a clearer more interwoven structure of 3MAA was attributed to evacuation of some volatile components of the parent beads after calcinations which led to the porosity development. Volatilization of matter on surfaces of mesoporous alumina after calcination leading to porosity development has been reported [13]. The morphological structure of PAA and 3MAA are presented in Fig. 2.

The spectrums for EDX of PAA and 3MAA and their corresponding elements detected are presented in Fig. 3.

Three distinctive peaks emerged in the spectrum of 3MAA as against two peaks found in the PAA EDX analysis as seen in Fig. 3. The third spectrum indicated the presence of sodium which was introduced during the modification process. An EDX analysis was used to show a percentage increase of Al content of a clay after pillaring with solution of aluminum [19].

The PAA poor crystalline structure with broad diffractometer peaks attributed to aluminum hydroxide in the form of bayerite ($\gamma\text{-AlO}(\text{OH})$) appeared at two different peaks 14.48 and 28.27 of 2θ . The 3MAA XRD diffractogram revealed distinct and sharp peaks in the form of boehmite appeared at 18.62 and 20.54 which were sodium aluminum oxide ($\text{Al}_2\text{Na}_2\text{O}_4$) compound attributed to modification with 30% NaOH. Distinct boehmite peaks of transition alumina of high crystalline peaks have been reported [21]. The more locally organized mesopore structures found in bayerites and its thermodynamic stability than boehmite which has no such structure, also enhanced adsorption of CO_2 on the adsorbent after modification and calcinations [22]. The XRD diffractogram is shown in Fig. 4.

The chemistry of CO_2 on a surface (adsorbent) is paramount for understanding its control from polluting the environment [23]. The five FTIR spectrums of PAA, 1MAA, 2MAA, 3MAA and 4MAA exhibited similar functional groups on certain wavenumbers as shown in Fig. 5. These include broad stretches between 2850 and 3500 cm^{-1} which were attributed to presence of some O–H or

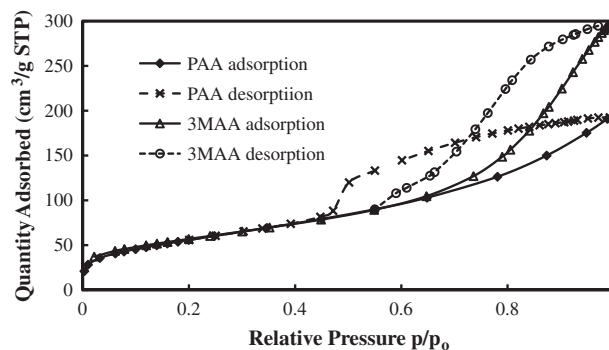


Fig. 1. Nitrogen adsorption–desorption isotherms for PAA and 3MAA.

N–H groups, some amide groups (N–H) groups peaks on 1647 cm^{-1} wavenumber, some $\text{C}\equiv\text{C}$ stretches of alkynes functional groups around 2106 cm^{-1} , and some C–H and C–N stretches around 1384 cm^{-1} band. Some distinct strong peaks at 1400 and 1500 cm^{-1} were found on spectrums of both PAA and 3MAA, these peaks were attributed to presence of some carboxylates and asymmetric nitro functional groups. The extra nitro-functional group on 3MAA coupled with its larger micropore volume that is, an adsorption system involving both physical and chemical activity may have contributed to the adsorbent adsorption capability [24,25].

3.2. Adsorbent modification parameter study

The modification of activated alumina adsorbent involved study of parameters such as percentage of sodium hydroxide (10–40%), calcinations temperatures (200–500 °C) and calcinations time (2–4 h) suitability. The influence of each parameter on the adsorbent modification was investigated for CO_2 capture through adsorption column experiment at certain fixed conditions such as adsorption temperature (35 °C), percentage of CO_2 (15%) in the feed (85% balance of N_2), total feed flow rate (90 mL/min), amount of adsorbent used (4 g) and adsorbent size (1–2 mm). Graphical representation of effect of percentage of sodium hydroxide, calcinations temperature and calcinations time on the activated alumina modification are shown in Fig. 6.

Chemical modification of the activated alumina involved the use of various percentages (10%, 20%, 30% and 40%) of NaOH and then calcined at fixed temperature and time obtained from preliminary investigation. The breakthrough profiles for various concentrations used are presented in Fig. 6(a). Adsorption of CO_2 using 3MAA gave the longest breakthrough time of 3.67 min while the unmodified adsorbent PAA had the shortest breakthrough time of 1.17 min which gave corresponding adsorption capacities of 51.92 and 19.61 mg/g. The longest breakthrough time of 3MAA was attributed to its developed porosity which was revealed by the nitrogen adsorption–desorption presented in Table 1. The CO_2 adsorption enhancement was also due to formation of carbonates between the carbon dioxide molecules and those of sodium on the surfaces of the modified activated alumina beads (3MAA) [26]. Other breakthrough times/adsorption capacities for 1MAA, 2MAA and 4MAA were 2.17 min/39.43 mg/g, 3.33 min/44.42 mg/g and 3.17 min/49.13 mg/g, respectively.

The effect of calcinations temperature variation on activated alumina modification was studied at 200, 300, 400 and 500 °C [16]. It was observed that the extension of breakthrough time was directly proportional to increase in calcinations temperature, the profiles are shown in Fig. 6(b). However, the difference in breakthrough time extension between 200 and 300 °C was not significant. It was attributed to insufficient heat at these temperatures that was required for development of the activated alumina

Table 1
Surface area and porosity distribution for plain (PAA) and modified (3MAA) activated alumina.

Parameters	PAA	3MAA
BET surface area (m^2/g)	207.14	203.32
Total pore volume (cm^3/g)	0.29	0.45
Average pore width (Å)	57.04	88.83

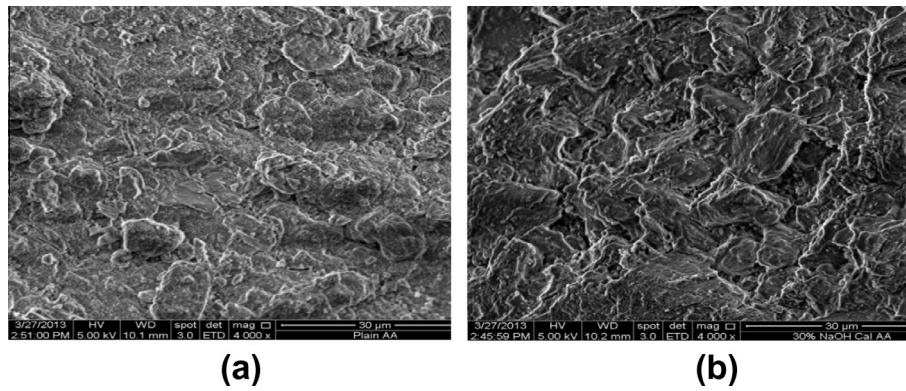


Fig. 2. SEM images of activated alumina at Mag. power of 2000× (a) PAA and (b) 3MAA.

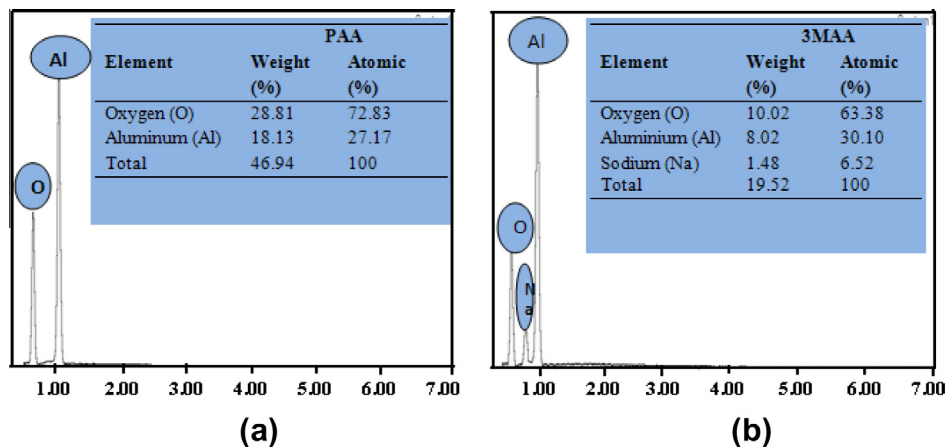


Fig. 3. The EDX spectrums of (a) unmodified and (b) modified activated alumina adsorbents.

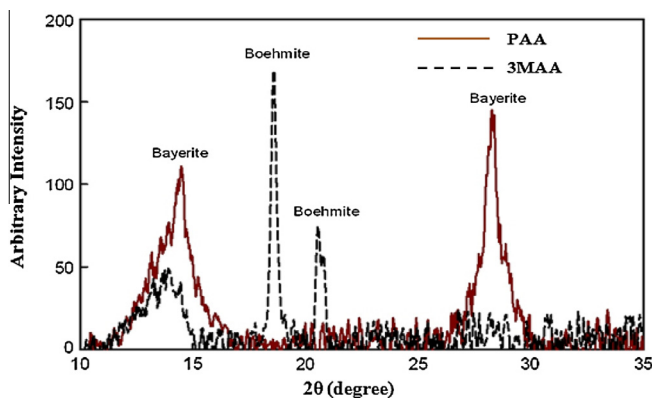


Fig. 4. The XRD spectrums of PAA and 3MAA.

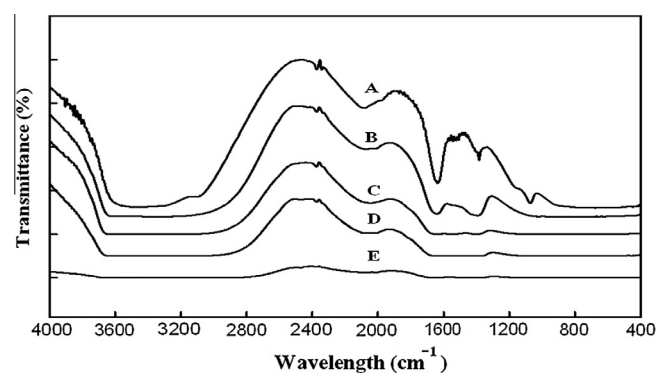


Fig. 5. The FTIR spectrums of (A) PAA, (B) 3MAA, (C) 1MAA, (D) 2MAA, and (E) 4MAA.

adsorbent. Modification of adsorbent for CO₂ capture at low temperature has been found to be kinetically slow and with smaller adsorption capacity [27]. The emergence of 500 °C as the optimum calcinations temperature was attributed to its suitability for removal of volatile components as well as moisture content from the adsorbent [13]. High calcinations was reported to have positively influenced the adsorption capacity increase [28].

The modified activated alumina was calcined at different duration (2, 3 and 4 h) to study the effect of time on the adsorbent modification for CO₂ capture. Breakthrough profiles for effect of calcinations time are shown in Fig. 6(c). Elongation of time of breakthrough point was found to increase with corresponding

increase of calcinations time. Longer calcinations time gave ample time for evacuation of some volatile impurities in the activated alumina beads leading to its porosity development. The 3MAA adsorbent calcined at 500 °C for 4 h led to its porosity development and gave the longest breakthrough time for CO₂ adsorption which implies better adsorption capacity. The 3MAA longer breakthrough period meant that the adsorbent took longer time to adsorb the CO₂ (adsorbate) before it was completely saturated or the adsorbent was capable of retaining the CO₂ at minimum effluent (C_t/C_0) concentration. It also meant that the 3MAA could be used for longer periods of CO₂ adsorption before regeneration or replacement [29].

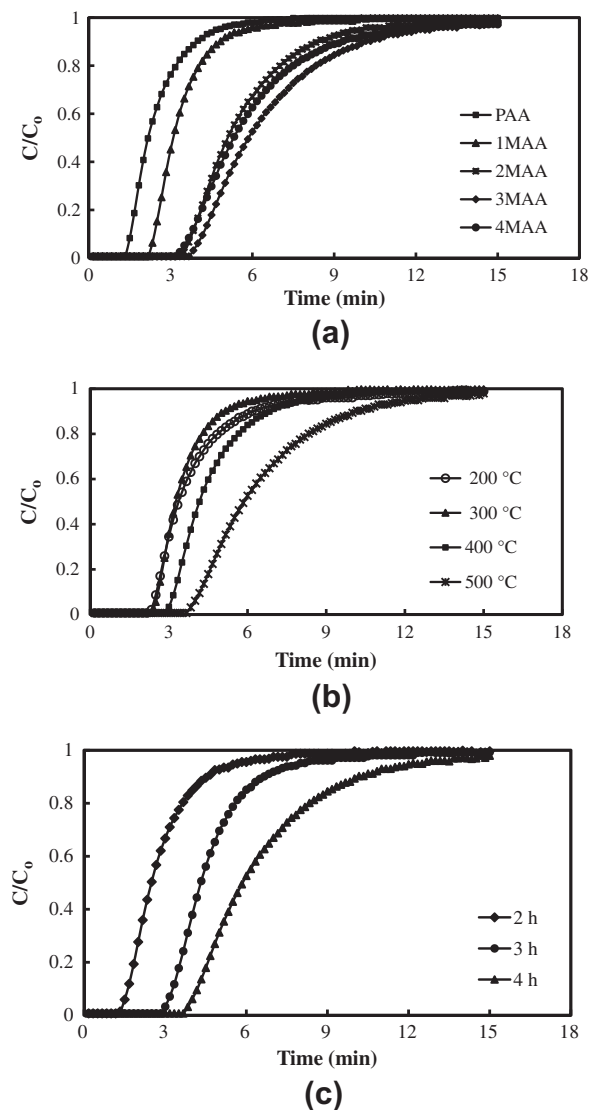


Fig. 6. Breakthrough curves for modified beads of activated alumina evaluated at (a) different percentage of NaOH, (b) different calcinations temperature, and (c) different calcinations time (calcinations time, 4 h; adsorption temperature, 35 °C; total feed flow rate, 90 mL/min; concentration of CO₂, 15%; amount of adsorbent, 4 g; size of beads, 1–2 mm).

3.3. Fixed-bed column parameter study

The adsorption of carbon dioxide on the modified activated alumina at optimum conditions of 30% NaOH, 500 °C for 4 h was studied by investigating the effects of five parameters namely: percentage of CO₂ in the feed, adsorption temperature, feed flow rate and bed depth.

3.3.1. Effect of percent carbon dioxide in the feed

The effect of variation (12%, 15% and 18%) of CO₂ in the feed (balance of N₂) on adsorption was investigated, the breakthrough profiles and adsorption capacities for the various percentage of CO₂ in the feed stream studied are presented in Fig. 7 and Table 2, respectively.

The percentage increase of CO₂ in the feed stream from 12% to 15% gave a corresponding adsorption increase from 24.64 to 51.92 mg/g. While a further increase of the CO₂ percentage in the feed to 18% negatively affected the adsorption capacity. At lower percentage concentration of CO₂ in the feed, the inflow sorbate

molecules were commensurate to the active sites on the adsorbent. While on the contrary, outrageous inflow of CO₂ molecules (18%) outstripped the limited available active sites on the adsorbent surface. Increase in percentage CO₂ in the feed increased the concentration gradient which has also been found by other researchers to overcome mass transfer resistance as well as increasing the adsorption capacity [30].

3.3.2. Effect of adsorption temperature

The temperature at which an adsorbent adsorb CO₂ is significant as that will determine its area of application whether in pre-combustion or post-combustion (from flue gases) units [24]. Adsorption of CO₂ by 3MAA was found to be decreasing as the temperature increased 51.92, 33.99 and 32.17 mg/g for temperatures of 35, 45 and 55 °C, respectively. This revealed that physisorption of CO₂ on 3MAA was dominant and this was attributed to the developed porosity of the adsorbent after modification. Similar observations of better adsorption of CO₂ at a lower column temperature due to association of alumina with sodium and also pore size development has been reported [6,27]. It can also be said that physisorption activities were negated as the adsorption temperature increased [13]. Other researchers [25] have observed contribution of nitrogen functionalities to CO₂ capture at room temperature, the extra nitrogen functional group on the 3MAA determined from FTIR analysis (Section 3.1) may have enhanced the adsorption at lower temperature investigated. Modification of the activated alumina with sodium hydroxide introduced some molecules of sodium on its surface which enhanced formation of sodium carbonate as CO₂ was adsorbed. This is similar to previous observations made that alkali metal carbonates can adsorb CO₂ at low adsorption temperatures [26,31]. The breakthrough curves for adsorption of CO₂ at different temperatures and their adsorption capacities are depicted in Fig. 8 and Table 2, respectively.

3.3.3. Effect of influent feed flow rate

The variation of the feed flow rate (90, 120 and 150 mL/min) into the adsorption column was synonymous with an increase in mass flow. At the slow flow rate of 90 mL/min, the breakthrough time was elongated as compared with the higher flow rate of 150 mL/min. Longer residence time experienced at lower flow rates allow for diffusion of molecules of the CO₂ which translated to higher adsorption capacity of 51.92 mg/g when compared with 40.14 and 37.64 mg/g for 120 and 150 mL/min, respectively. Early saturation of adsorption column adsorbent bed was associated with higher mass transfer coefficient emanating from high flow rate [32]. Adsorption capacities and breakthrough profiles for various feed flow rate effects are presented in Table 2 and Fig. 9, respectively.

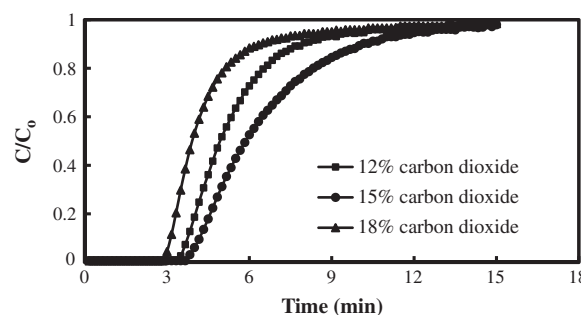


Fig. 7. Breakthrough curves for modified beads activated alumina evaluated at different percent concentration of CO₂ in the feed (modification with 30% NaOH; calcinations time, 4 h; adsorption temperature, 35 °C; total feed flow rate, 90 mL/min; concentration of CO₂, 15%; amount of beads, 4 g; size of beads, 1–2 mm).

Table 2
Breakthrough time and adsorption capacity for parameters investigated.

Parameters	Values	Breakthrough time (s)	Adsorption capacity (mg/g)
CO ₂ % in the feed	12	200	24.64
	15	220	51.92
	18	170	33.01
Adsorption temperature (°C)	35	220	51.92
	45	190	33.99
	55	160	32.17
Feed flow rate (mL/min)	90	220	51.92
	120	120	40.14
	150	70	37.64
Amount of adsorbent in the adsorption column (g)	2	80	36.65
	4	220	51.92
	6	450	54.81

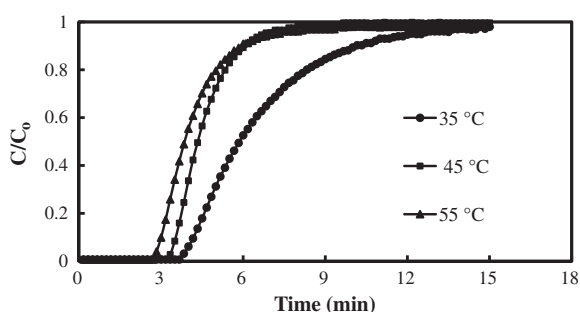


Fig. 8. Breakthrough curves for modified beads activated alumina evaluated at different adsorption temperature (modification with 30% NaOH; calcinations time, 4 h; calcinations temperature, 500 °C; total feed flow rate, 90 mL/min; concentration of CO₂, 15%; amount of beads, 4 g; size of beads, 1–2 mm).

3.3.4. Effect of amount of 3MAA in fixed-bed adsorption column

The breakthrough curves for variation in the amount of the 3MAA (2, 4 and 6 g) loaded into the adsorption column on CO₂ adsorption and the adsorption capacities obtained are shown in Fig. 10 and Table 2, respectively. An increase in the amount of adsorbent was accompanied with subsequent increase in the service area of the adsorbent. The service area increase enhanced more contact between the active sites on the 3MAA and CO₂ molecules, thus increasing the adsorption capacity. It is also interesting to note that enlarged service area increased the volume of synthetic flue gas (CO₂/N₂ mixture) treatment as well as gave a prolonged breakthrough point attainment.

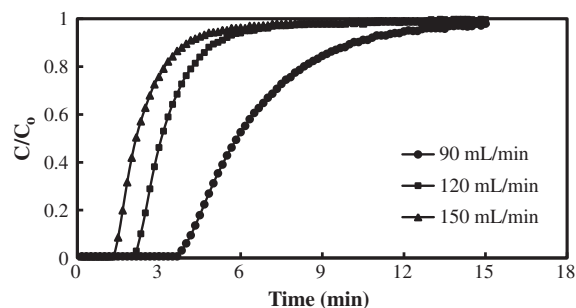


Fig. 9. Breakthrough curves for CO₂ adsorption by 3MAA evaluated at different total flow rate (modification with 30% NaOH; calcinations time, 4 h; adsorption temperature, 35 °C; total feed flow rate, 90 mL/min; concentration of CO₂, 15%; amount of beads, 4 g; size of beads, 1–2 mm).

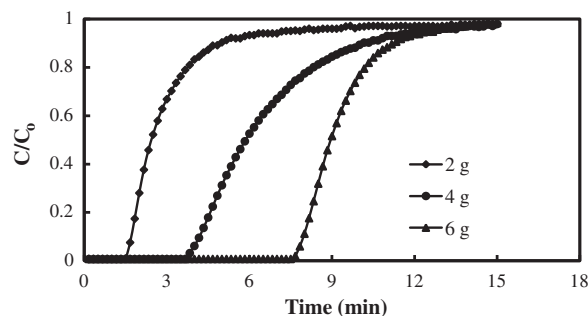


Fig. 10. Breakthrough curves for 3MAA evaluated at different amount of the beads used (modification with 30% NaOH; calcinations time, 4 h; adsorption temperature, 35 °C; total feed flow rate, 90 mL/min; concentration of CO₂, 15%; calcinations temperature, 500 °C; particle size of 1–2 mm).

3.4. Comparison of alumina sorption capacities for CO₂ adsorption

Modification of activated alumina with 30% sodium hydroxide calcined at 500 °C for 4 h gave about 164.76% increase in adsorption capacity of CO₂ when compared with the commercial plain activated alumina adsorbent. The significant increase in CO₂ adsorption capacity was attributed to the increased basicity by the NaOH which gave rise to the pore width as well as total pore volume development as discussed earlier in Section 3.1. The adsorption capacities obtained in this study are comparable with results reported by other researchers as can be seen summarized in Table 3.

3.5. Desorption of modified activated alumina (3MAA) adsorbent

Desorption was carried out by reheating the 3MAA to a desorption temperature (110 °C) which was similar to the adsorbent pretreatment column temperature (110 °C). The temperature 110 °C was found to be suitable for complete CO₂ desorption from the 3MAA and the desorption breakthrough profiles are presented in Fig. 11. This method is in accordance with report by previous researchers that successfully carried out desorption at a temperature similar to the adsorbent pretreatment temperature [28]. The ease of desorption of the adsorbed CO₂ molecules from the 3MAA was attributed to initial predominant physical adsorption into the pore volume of the CO₂. The three cycles of adsorption after desorption of 3MAA gave adsorption capacities of 42.81, 35.76 and 35.24 mg/g for first, second and third cycles. The significant difference between the first and other adsorption capacities of second and third cycles was attributed to blockages of 3MAA pores by some chemisorbed CO₂ molecules on nitrogen active sites and with some residual sodium on the surface (forming carbonates) before the predominance of physisorption activities [36]. Similar observation has been reported on desorption of CO₂ on N-doped mesoporous alumina [13]. Reusability of CO₂ has been undertaken by other researchers in order to cut cost of adsorption through minimizing the frequency of replacement of adsorbents and the use of energy [12].

4. Conclusion

Modification of activated alumina was successfully carried out with 30% concentration of sodium hydroxide after calcinations at 500 °C for 4 h. The fixed-bed column adsorption parameters investigated revealed that concentration of CO₂ in the feed of 15%, total feed flow rate of 90 mL/min, adsorption temperature of 35 °C and 4 g of 3MAA were suitable for the CO₂ capture. The modified PAA (3MAA) surface had its total pore volume and average pore width

Table 3
Comparison of adsorption capacity of alumina based adsorbent for CO₂ capturing.

Adsorbent	CO ₂ % in the feed	Adsorption temperature (°C)	Feed flow rate (mL/min)	Adsorption capacity (mg CO ₂ /g)	Reference
PAA	15.00	35	90	19.61	Present work
3MAA	15.00	35	90	51.92	Present work
Commercial MA ^a SASOL	15.40	55	52	7.45	[13]
Chitosan based MA ^a	15.40	55	52	29.40	[13]
MA ^a commercial	15.85	75	10	52.00	[12]
PEI ^b impregnated MA ^a	15.85	25	10	120.00	[12]
Sodium oxide promoted alumina	16.00	225	–	16.72	[6]
Palm shell-based activated carbon (AC)	30	40–50	15	37.10	[33]
2-Amino-2-methyl-1-propanol AC	30	40–50	15	64.00	[33]
2-Amino-2-methyl-1,3-propanediol AC	30	40–50	15	54.00	[33]
2-(Methylamino) ethanol AC	30	40–50	15	44.00	[33]
3-[2-(2-Aminoethylamino)ethylamino]propyl-trimethoxysilane modified MgAl layered double hydroxide	–	80	–	78	[34]
MgO-based adsorbent, 5A3M	10	200	50	44	[35]
MgO-based adsorbent, 5A5M	10	200	50	77	[35]
MgO-based adsorbent, 5A7M	10	200	50	37	[35]

^a MA is mesoporous alumina.

^b PEI is polyethylenimine.

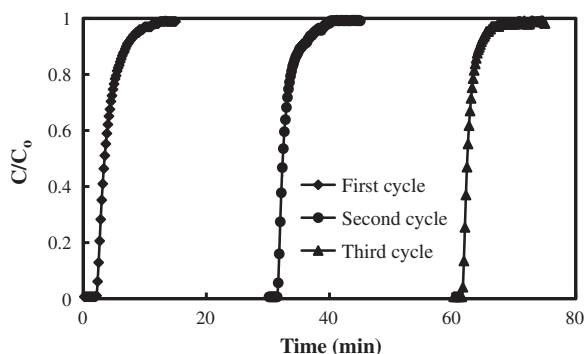


Fig. 11. Breakthrough curves for 3MAA adsorption–desorption (Calcinations time, 4 h; adsorption temperature, 35 °C; total feed flow rate, 90 mL/min; concentration of CO₂, 15%; calcinations temperature, 500 °C; amount of 3MAA 4 g; particle size 1–2 mm).

developed and also had nitrogen functionalities which promoted physisorption and chemisorption mechanism of adsorption of the CO₂ on it. The adsorption–desorption test of 3MAA showed that the adsorbent can be reused successfully for three cycles. The results of this study revealed that activated alumina can be used to remedy CO₂ pollution in the environment.

Acknowledgments

The authors acknowledge the research grant provided by the Ministry of Science, Technology and Innovation (MOSTI), Malaysia under Science Fund grant (Project no: 06-01-05-SF0513), that resulted in the article.

References

- [1] A. Duffy, G.M. Walker, S.J. Allen, Investigations on the adsorption of acidic gases using, activated dolomite, *Chem. Eng. J.* 117 (2006) 239–244.
- [2] V.P. Mulgundmath, R.A. Jones, F.H. Tezel, J. Thibault, Fixed bed adsorption for the removal of carbon dioxide from nitrogen: breakthrough behaviour and modelling for heat and mass transfer, *Sep. Purif. Technol.* 85 (2012) 17–27.
- [3] Y. Zhao, Y. Shen, L. Bai, Effect of chemical modification on carbon dioxide adsorption, property of mesoporous silica, *J. Colloid Interface Sci.* 379 (2012) 94–100.

- [4] J.-R. Li, Y. Ma, M.C. McCarthy, J. Sculley, J. Yu, H.-K. Jeong, P.B. Balbuena, H.-C. Zhou, Carbon dioxide capture-related gas adsorption and separation in metal-organic frameworks, *Coord. Chem. Rev.* 255 (2011) 1791–1823.
- [5] A.E. Amooghin, H. Sanaeepur, A. Moghadassi, A. Kargari, D. Ghanbari, Z.S. Mehrabadi, Modification of ABS membrane by PEG for capturing carbon dioxide from CO₂/N₂ Streams, *Sep. Sci. Technol.* 45 (2010) 1385–1394.
- [6] M. Li, Dynamics of CO₂ adsorption on sodium oxide promoted alumina in a packed-bed, reactor, *Chem. Eng. Sci.* 66 (2011) 5938–5944.
- [7] B. Guo, L. Chang, K. Xie, Adsorption of carbon dioxide on activated carbon, *J. Nat. Gas Chem.* 15 (2006) 223–229.
- [8] R. Serna-Guerrero, A. Sayari, Modeling adsorption of CO₂ on amine-functionalized mesoporous silica. 2: Kinetics and breakthrough curves, *Chem. Eng. J.* 161 (2010) 182–190.
- [9] T.L.P. Dantas, F.M.T. Luna, I.J. Silva Jr., D.C.S. de Azevedo, C.A. Grande, A.E. Rodrigues, R.F.P.M. Moreira, Carbon dioxide–nitrogen separation through adsorption on activated carbon in a fixed bed, *Chem. Eng. J.* 169 (2011) 11–19.
- [10] Y. Labreche, R.P. Lively, F. Rezaei, G. Chen, C.W. Jones, W.J. Koros, Post-spinning infusion of poly(ethyleneimine) into polymer/silica hollow fiber sorbents for carbon dioxide capture, *Chem. Eng. J.* 221 (2013) 166–175.
- [11] M.S. Shafeeyan, W.M.A.W. Daud, A. Houshmand, A. Shamiri, A review on surface modification of activated carbon for carbon dioxide adsorption, *J. Anal. Appl. Pyrolysis* 89 (2010) 143–151.
- [12] C. Chen, W.-S. Ahn, CO₂ capture using mesoporous alumina prepared by a sol-gel process, *Chem. Eng. J.* 166 (2011) 646–651.
- [13] J.A. Thote, R.V. Chatti, K.S. Iyer, V. Kumar, A.N. Valechha, N.K. Labhsetwar, R.B. Biniwale, M.K.N. Yenkie, S.S. Rayalu, N-doped mesoporous alumina for adsorption of carbon dioxide, *J. Environ. Sci.* 24 (2012) 1979–1984.
- [14] H.-J. Sedjame, G. Lafaye, J. Barbier Jr, N-butanol removal over alumina supported platinum catalysts, *Appl. Catal. B: Environ.* 132–133 (2013) 132–141.
- [15] T.L.P. Dantas, F.M.T. Luna, I.J. Silva Jr, A.E.B. Torres, D.C.S. de Azevedo, A.E. Rodrigues, R.F.P.M. Moreira, Carbon dioxide–nitrogen separation through pressure swing adsorption, *Chem. Eng. J.* 172 (2011) 698–704.
- [16] G.K. Chuah, S. Jaenicke, T.H. Xu, The effect of digestion on the surface area and porosity of alumina, *Micropor. Mesopor. Mater.* 37 (2000) 345–353.
- [17] R.P. Vijayalakshmi, R.V. Jasra, S.G.T. Bhat, Modification of texture and surface basicity of γ -alumina by chemical treatment, *Recent Adv. Basic Appl. Aspects Ind. Catal.* 113 (1998) 613–622.
- [18] H. Wu, L. Chen, G. Gao, Y. Zhang, T. Wang, S. Guo, Treatment effect on the adsorption capacity of alumina for removal fluoride, *Nano Biomed. Eng.* 2 (2010) 231–235.
- [19] O.B. Ayodele, J.K. Lim, B.H. Hameed, Pillared montmorillonite supported ferric oxalate as heterogeneous photo-Fenton catalyst for degradation of amoxicillin, *Appl. Catal. A: Gen.* 413–414 (2012) 301–309.
- [20] K.S.W. Sing, D.H. Everett, R.A.W. Haul, L. Moscou, R.A. Pierotti, J. Rouquerol, T. Siemieniowska, Reporting Physisorption Data for Gas/Solid Systems with Special Reference to the Determination of Surface Area and Porosity, vol. 57, International Union of Pure and Applied Chemistry, Physical Chemistry Division, Commission on Colloid and Surface Chemistry Including Catalysis, 1985.
- [21] M.S.M. Yusoff, M. Muslimin, Synthesis of alumina using the solvothermal method, *The Malaysian J. Analyt. Sci.* 11 (2007) 7.
- [22] W.Q. Jiao, M.B. Yue, Y.M. Wang, M.-Y. He, Synthesis of morphology-controlled mesoporous transition aluminas derived from the decomposition of alumina hydrates, *Micropor. Mesopor. Mater.* 147 (2012) 167–177.

- [23] J. Baltrusaitis, J. Schuttlefield, E. Zeitler, V.H. Grassian, Carbon dioxide adsorption on oxide nanoparticle surfaces, *Chem. Eng. J.* 170 (2011) 471–481.
- [24] M.G. Plaza, C. Pevida, A. Arenillas, F. Rubiera, J.J. Pis, CO₂ capture by adsorption with nitrogen enriched carbons, *Fuel* 86 (2007) 2204–2212.
- [25] M.S. Shafeeyan, W.M.A.W. Daud, A. Houshmand, A. Arami-Niya, Ammonia modification of activated carbon to enhance carbon dioxide adsorption: effect of pre-oxidation, *Appl. Surf. Sci.* 257 (2011) 3936–3942.
- [26] C. Zhao, X. Chen, E.J. Anthony, X. Jiang, L. Duan, Y. Wu, W. Dong, C. Zhao, Capturing CO₂ in flue gas from fossil fuel-fired power plants using dry regenerable alkali metal-based sorbent, *Progress Energy Combust. Sci.* (2013). <http://dx.doi.org/10.1016/j.pecs.2013.05.001>.
- [27] C. Pevida, T.C. Drage, C.E. Snape, Silica-templated melamine–formaldehyde resin derived adsorbents for CO₂ capture, *Carbon* 46 (2008) 1464–1474.
- [28] O. Aschenbrenner, P. McGuire, S. Alsamaq, J. Wang, S. Supasitmongkol, B. Al-Duri, P. Styring, J. Wood, Adsorption of carbon dioxide on hydrotalcite-like compounds of different compositions, *Chem. Eng. Res. Des.* 89 (2011) 1711–1721.
- [29] M. Auta, B.H. Hameed, Coalesced chitosan activated carbon composite for batch and fixed-bed adsorption of cationic and anionic dyes, *Colloids Surf. B. Biointerfaces* 105 (2013) 199–206.
- [30] N. Chen, Z. Zhang, C. Feng, M. Li, R. Chen, N. Sugiura, Investigations on the batch and fixed-bed column performance of fluoride adsorption by Kanuma mud, *Desalination* 268 (2011) 76–82.
- [31] S.C. Lee, B.Y. Choi, T.J. Lee, C.K. Ryu, Y.S. Ahn, J.C. Kim, CO₂ absorption and regeneration of alkali metal-based solid sorbents, *Catal. Today* 111 (2006) 385–390.
- [32] K. Munusamy, G. Sethia, D.V. Patil, P.B. Somayajulu Rallapalli, R.S. Somani, H.C. Bajaj, Sorption of carbon dioxide, methane, nitrogen and carbon monoxide on MIL-101(Cr): volumetric measurements and dynamic adsorption studies, *Chem. Eng. J.* 195–196 (2012) 359–368.
- [33] C.S. Lee, Y.L. Ong, M.K. Aroua, W.M.A.W. Daud, Impregnation of palm shell-based activated carbon with sterically hindered amines for CO₂ adsorption, *Chem. Eng. J.* 219 (2013) 558–564.
- [34] J. Wang, L.A. Stevens, T.C. Drage, J. Wood, Preparation and CO₂ adsorption of amine modified Mg–Al LDH via exfoliation route, *Chem. Eng. Sci.* 68 (2012) 424–431.
- [35] K.K. Han, Y. Zhou, Y. Chun, J.H. Zhu, Efficient MgO-based mesoporous CO₂ trapper and its performance at high temperature, *J. Hazard. Mater.* 203–204 (2012) 341–347.
- [36] C.-F. Mao, M.A. Vannice, High surface area cu-alumina. I. Adsorption properties and heats of adsorption of carbon monoxide, carbon dioxide, and ethylene, *Appl. Catal. A: Gen.* 111 (1994) 151–173.